# Detection of a Hypercharge Axion in ATLAS

a Monte-Carlo Simulation of
a Pseudo-Scalar Particle (Hypercharge Axion)
with Electroweak Interactions
for the ATLAS Detector
in the Large Hadron Collider at CERN

Erik Elfgren
elf@ludd.luth.se

December, 2000
Division of Physics
LuleåUniversity of Technology
Luleå, SE-971 87, Sweden
http://www.luth.se/depts/mt/fy/

**Abstract**

This Master of Science thesis treats the hypercharge axion, which is a hypothetical pseudo-scalar particle with electroweak interactions.

First, the theoretical context and the motivations for this study are discussed. In short, the hypercharge axion is introduced to explain the dominance of matter over antimatter in the universe and the existence of large-scale magnetic fields.

Second, the phenomenological properties are analyzed and the distinguishing marks are underlined. These are basically the products of photons and $Z^0$s with high transverse momenta and invariant mass equal to that of the axion.

Third, the simulation is carried out with two photons producing the axion which decays into $Z^0$s and/or photons. The event simulation is run through the simulator ATLFAST of ATLAS (A Toroidal Large Hadron Collider ApparatuS) at CERN.

Finally, the characteristics of the axion decay are analyzed and the criteria for detection are presented. A study of the background is also included. The result is that for certain values of the axion mass and the mass scale (both in the order of a TeV), the hypercharge axion could be detected in ATLAS.

# Preface

This is a Master of Science thesis at the Luleå University of Technology, Sweden. The research has been done at Université de Montréal, Canada, under the supervision of Professor Georges Azuelos. My thesis receiver in Sweden has been Professor Sverker Fredriksson.

The thesis is divided into three chapters. The first one treats the motivations for the hypercharge axion and some theoretical background. The second covers the preparations and simulations as well as some predictions from the theory. The third chapter contains the results of the simulations and some conclusions.

Notations and units: In the calculations we use units where Planck's constant, the speed of light and Boltzmann's constant are all equal to unity. A bar over a particle name signifies the antiparticle. The word axion is interchangeable with hypercharge axion. Footnotes are used to explain further, but are not necessary for the basic comprehension. If a word is marked in *slanted* it is either supposed to be known, or is *curiosum*. These words are explained in the Glossary in Appendix A. All symbols, abbreviations and constants used in the thesis are listed and briefly explained in Appendix B.

Finally I would like to express my deep gratitude to all the people that have helped on the different subjects of this thesis. First of all to my supervisor Georges Azuelos, Université de Montréal, for his eternal patience with all my questions as well as numerous suggestions and good discussions. I would also like to thank Gilles Coutures, Université de Québec de Montréal, who has been a great help and who made the theoretical work leading to this thesis. I thank my professor in Sweden, Sverker Fredriksson, Luleå University of Technology, for his support and all our previous discussions that have helped me in this work. As for the motivations for the hypercharge axion, I would like to thank Roger MacKenzie, Robert Brandenberger, James Cline, and Salman Habib for interesting discussions on cosmology, sphalerons and electroweak baryogenesis.

Montréal in December 2000, Erik Elfgren.

# Contents

# Introduction

Ever since the discovery of antimatter it has been a mystery that almost all of our experiments in particle physics are symmetric in matter and antimatter, but yet the universe seems to be constituted entirely of matter. Some general conditions were outlined by Sakharov in 1967, but the problem itself remains unsolved.

The first possible explanations were based on the grand unified theories (GUTs) in which the asymmetry was generated very close to big bang. These theories allow baryon-to-lepton decay, which could generate an asymmetry. One drawback is that the theories cannot be tested without tremendous amounts of energy ($\gtrsim 10^{16}$ GeV), far beyond our reach.

Later on, theories evolved that could explain the generation of the asymmetry without GUT theories. Most of them suppose that the asymmetry was created around the electroweak phase transition at $T \sim 100$ GeV when the electroweak symmetry was broken. Supersymmetric theories can offer possible explanations under certain conditions, but the standard model itself seems incapable to produce the required asymmetry.

A theory proposed by Brustein and Oaknin is particularly appealing for several reasons. It suggests simply that the introduction of a scalar field could create the required asymmetry through coupling to the hypercharge. As a bonus, the theory could also explain the existence of large magnetic fields in cosmic plasmas. The pseudoscalar was named hypercharge axion from its couplings to hypercharge.

In summary, the hypercharge axion can possibly explain the dominance of matter over antimatter in the universe. In other words, why we exist!

Finally, the hypercharge axion is expected to have a mass in the TeV range, making it possible to detect in the ATLAS detector at the large hadron collider (LHC) which is now constructed at CERN, Geneva, and will be operational by 2005. This is the subject of this masters thesis.

Some references on particle physics are Nash [1], Peskin and Schroeder [2], and the CERN photo-gallery: http://press.web.cern.ch/Press/Photos/.

# Chapter 1

# Background and Motivations

This chapter treats the background to my research, why it may be of interest to study the axion and what has been done so far. Briefly, the axion could be the reason for the mysterious domination of matter over antimatter in the universe. Before introducing the axion some theory is presented to situate it in its context and explain how the axion can be the reason behind the domination of matter.

This chapter is divided into three major parts. The first one addresses some general questions, such as how we can be sure that the universe really has more matter than antimatter, and some very general conditions that must be fulfilled for the asymmetry to exist. These conditions are called the Sakharov criteria and they must be fulfilled for statistical reasons.

The second part of this chapter is devoted to *baryogenesis*, i.e., the process by which the asymmetry is created. The subject is very complicated, so I will content myself with a rather qualitative description of the different phenomena. Among these are the *electroweak phase transition*, which took place about $10^{-10}$ seconds after the big bang; the role of hypermagnetic fields in the phase transition; sphalerons which counter asymmetries and the Chern-Simons number, which is directly proportional to the baryon asymmetry.

The third part treats the axion itself, with the properties proposed by Brustein and Oaknin [3]. A description of how the axion could amplify the hypermagnetic fields is included as well as the couplings and branching ratios. A discussion of where the hypercharge axion could appear is also provided. Its properties are compared to those of particles in the most popular extensions of the standard model: the minimal supersymmetric model and superstring models.

## 1.1 Matter-Antimatter Asymmetry

### 1.1.1 How do we know that the Universe is Asymmetric?

While our theories in particle physics are very nearly symmetric in matter-antimatter (almost all relevant experiments in particle physics show this behavior), the universe itself is far from being so. We have several reasons to believe that the universe is mainly constituted of matter. The most obvious reason is that we have explored our solar system without annihilating, which would not have been the case if there had been antimatter in significant abundance in our solar system.

To conclude that the universe at large is made of matter is not as obvious. What if another part of our galaxy, or another galaxy nearby were constituted of antimatter? This possibility is improbable since cosmic radiation in that case should contain antimatter. Cosmic radiation does contain some antiprotons, but that fraction ($10^{-4}$) is well explained by the reaction $p+p \rightarrow 3p+\bar{p}$, which has nothing to do with the eventual existence of larger chunks of antimatter. This is evidence that there is no large antimatter cluster in our relative proximity.

As for more distant galaxies, we should see gamma-ray emissions from the interface between matter and antimatter galaxies. The gamma rays should have an energy up to that of a particle-antiparticle pair. These gamma rays should produce a detectable background, which is not observed. Causality is not an argument against this either, as we can see (almost) all parts of the universe, only at different times. The separation should have occurred rather early for any significant amount of antimatter to remain, so that we should observe gamma rays from these parts too. Thus, there is a negligible amount of antimatter on the scale of clusters. For the interested reader, references like Steigman [5], Stecker [6] and Cohen et al. [7] are recommended.

### 1.1.2 How did the Universe become Asymmetric?

The first possiblility is that the universe started asymmetric. This is not a very interesting possibility because of its sterility. It does not suggest any new physics, nor any "real" explanations or predictions. Besides, it is in contradiction with inflation theory, which says that any initial abundances are diluted.

The second possibility is that the universe started symmetric (or at least became symmetric at a rather early stage, e.g. during inflation), but the symmetry was broken through some mechanism. For the baryon asymmetry this

mechanism is called baryogenesis. Note that even though baryon number and lepton number separately are violated, the difference $B - L$ is thought to be constant.

The imbalance in the amount of matter and antimatter can basically be measured as the imbalance in the amount of baryons and antibaryons, since baryons (neutrons and protons) are the heaviest of the basic constituents of normal matter. Also, we cannot measure the lepton asymmetry because we know neither how many neutrinos there are in the universe, nor their mass. The asymmetry is often characterized by the baryon-to-entropy ([20], page 133) ratio:

$$\eta = \frac{n_B}{s} = \frac{n_b - n_{\bar{b}}}{s} \approx 10^{-10}, \tag{1.1}$$

which can be seen as the the ratio between the number of baryons and the number of photons (which come from the annihilation of matter and antimatter).

In 1967, Sakharov [8] stated that there are three criteria that must be satisfied to explain the present matter-antimatter asymmetry:

1. **Non-conservation of baryons**
   If the baryon number is conserved in all reactions then the observed asymmetry can only reflect asymmetric initial conditions. Hence, there must have existed some process that violated the baryon number. Grand unified theories (GUTs) have leptons and quarks in the same representation, and therefore allow decay of baryons to leptons. A process that has been searched for is proton decay to positron, $p \to e^+\nu_e$, but no evidence for such processes has been found so far. However, baryon number violation can also be obtained from anomalies, which can occur without any extension from the standard model, see below.

2. **Charge ($C$) and Charge-Parity ($CP$) violation**
   *$CP$ symmetry* implies that if there are two identical *decay channels*, except that one involves matter and the other involves antimatter, then both happen with equal probability, e.g., $P(e^-p^+ \to n\nu) = P(e^+\bar{p} \to \bar{n}\bar{\nu})$. In other words, if $CP$ symmetry is violated and if you could contact someone in another part of the universe you could instruct him how to make an experiment to tell whether he is made of matter or antimatter. Without a preference for matter or antimatter, baryon non-conservation would work as much one way as the other, and matter and antimatter would have annihilated.

3. **Thermodynamic nonequilibrium**
   The universe must have evolved from a state of thermodynamic equilibrium to thermodynamic nonequilibrium. This is necessary because in thermodynamic equilibrium the net number density of baryons is equal to that of antibaryons. This can be illustrated as follows. In thermodynamic equilibrium the number density $n(E)$ of a particle is given by

$$n(E) \propto e^{-k_B H/T}, \tag{1.2}$$

   where $k_B$ is Boltzmann constant, $T$ is the temperature and $H$ is the Hamiltonian of the system. Now, due to the Charge-Parity-Time ($CPT$) theorem [10] the masses of particles and antiparticles are the same[1], which means that the Hamiltonians are the same. In other words, equation (1.2) implies that in thermodynamic equilibrium, the number (density) of baryons is the same as the number (density) of antibaryons. You can also explain this condition with the fact that a difference in the number of particles and antiparticles decreases the randomness of the system, which is prohibited in thermodynamic equilibrium, as the second law of thermodynamics states that the entropy of a system must increase, or at best stay the same.

   One way of bringing the universe out of thermodynamic equilibrium is by a phase transition. However, the thermodynamic nonequilibrium needs to be very strong to allow the current asymmetry between matter and antimatter. A second-order phase transition is charaterized by continuously varying parameters, giving a weak thermodynamic nonequilibrium. A first-order phase transition has discontinuously varying parameters. To create the currently observed matter-antimatter asymmetry, a *strong* first-order phase transition is needed.

In summary, the entire production of the asymmetry should go trough the following steps (assuming the simplest procedure):

1. The universe started symmetric in matter and antimatter.
2. Processes violating baryon number, $C$ and $CP$ symmetry came into action.
3. The universe was (temporarily) brought out of thermodynamic equilibrium, allowing for an asymmetry between matter and antimatter to develop.

[1] The validity of the $CPT$ theorem is very fundamental, but is nevertheless questioned, see for example Eades and Hartman [11].

4. Very shortly after (or during) the return to thermodynamic equilibrium the baryon number violating processes stopped (otherwise the return to thermodynamic equilibrium would once again have brought the universe to symmetry between matter and antimatter).

5. The remaining matter and antimatter annihilated (into photons) until only the surplus matter remained.

## 1.2 Electroweak Model of Baryogenesis

In the minimal standard model, two of the Sakharov criteria are problematic. First, the high mass of the Higgs boson seems to preclude a first-order phase transition [4], which would have been a natural way to bring the universe out of thermodynamic equilibrium. Second, the CP violation is too weak to produce the observed baryon-to-photon ratio $10^{-10}$. This means that extensions of the standard model need to be considered, but before doing that an explanation of how the asymmetry can be created is appropriate.

Baryogenesis should take place sometimes very early in the history of the universe, in the first fractions of a second, before the formation of compounds of quarks like baryons and mesons (note that "free" quarks also have a baryon number).

As the baryogenesis must take place in thermodynamic nonequilibrium, there are two basic possibilities to investigate. First of all, the pure expansion of the universe provokes a thermodynamic nonequilibrium. However, at the time around the electroweak phase transition this has been estimated to be by far too weak to stop the symmetry from being restored. Second, the thermodynamic nonequilibrium can be caused by a phase transition, like the electroweak phase transition $10^{-10}$ seconds after the Big Bang. Thus the thermodynamic nonequilibrium must either be caused by a phase transition, or occur at a very early stage at the scale of the grand unified theories (GUTs). In this study, the electroweak phase transition will be treated in further detail.

Some aspects of the GUT thermodynamic nonequilibrium can be found in Kolb and Wolfram [9].

### 1.2.1 Analogy with a Pendulum

For several of the concepts introduced in the following sections, an analogy with a mechanical pendulum can be of great help. The Lagrangian of the

pendulum is:

$$L = \tfrac{1}{2}ml^2\dot{\theta}^2 - mgl(1 - \cos\theta), \tag{1.3}$$

where $m$ is the mass and $l$ is the length of the pendulum ($\theta$ is the angle of inclination of the pendulum with respect to the vertical and $g \approx 9.8$ m/s$^2$ is the standard acceleration of gravity).

The system is periodic and the periodicity can be labeled by an integer $n$:

$$\theta_n = 2n\pi. \tag{1.4}$$

Below is a list of concepts that have anlogues for the electroweak phase transition:

**Winding number** The number of rotations, $n$.

**Vacuum** The solution where the pendulum is at rest ($\theta = 0$).

**Sphaleron** The solution where the pendulum is at its highest point ($\theta = \pi$). Sphaleron is also often used as a label of a rotation, passing the sphaleron point, going to an adjacent winding number $n$. The energy of the sphaleron point is $mgl(1 - \cos\pi) = 2mgl$.

**Instanton** The tunneling of the pendulum from one winding number to the adjacent one. (This is a quantum mechanical effect and does not really make sense in this mechanical context, but it is included for completeness.)

**Thermal energy** A set of pendula having a randomly distributed energy, but with the mean energy equal to the thermal energy.

If the thermal energy becomes comparable to the sphaleron energy, it becomes possible for thermal transitions over the energy barrier to occur. The rate of these transitions can be calculated to be

$$\Gamma(T) \propto e^{-E_{sph}/T}, \tag{1.5}$$

so that when $T \sim E_{sph}$ the transitions between different vacua (different winding numbers) happen unhindered.

Another analogy between the pendulum and quantum field theory is that for low $T$, i.e., $\theta \approx 0$, we can approximate $\cos\theta \approx 1 - \theta^2/2$, which is the same thing as perturbation theory, which also is a kind of Taylor expansion around a minimum in the potential. However, in both cases information about the periodic structure of the system is lost.

### 1.2.2 Thermodynamic Nonequilibrium

This is the era when the Higgs first acquired a vacuum expectation value (vev), so the $Z^0$ and $W^{\pm}$ acquired masses. The temperature of the universe was at this stage of the order of 100 GeV.

As mentioned earlier, the phase transition has to be of first-order to induce a thermodynamic nonequilibrium strong enough. In fact, it is not even sufficient with a first order phase transition, but a *strong* first order phase transition is required in the simplest model.

The dynamics of the phase transition is obviously very important, and the imagined procedure is in analogy with that of pressurized boiling water. Close to a critical temperature $T_c$, "bubbles" of the other phase starts to form. These are regions of space where the electroweak symmetry is broken. For a start these bubbles die out as fast as they appear, but then they grow fast enough to form nucleates (called critical bubbles) and they expand and eventually fill the entire universe. At the bubble walls there is a significant departure from thermodynamic equilibrium.

### 1.2.3 Nonconservation of Baryon Number

Classically[2] the Lagrangian conserves both the baryon number and the lepton number. However, there are triangle anomalies (see figure 1.1), which add radiative corrections to the Lagrangian. The theory can be renormalized with conservation of either the vector *or* the *axial current*, but not both. We know very well that the vector current is conserved (by conservation of charge), which means that the axial current is not conserved. Now the integral over time of the divergence of the axial current (along with the conservation of the vector current) implies a change in baryon number.[3]

However, the radiative corrections from the anomalies are non-perturbative and at the temperature of the universe today, the corrections are extremely small. In the case of the pendulum above, they correspond to a thermal excitation such that the pendulum would pass its highest point, the *sphaleron*, or they correspond to *instanton* tunneling.

As in the case of the pendulum above, there is also a *winding number* associated with the Lagrangian, the *Chern-Simons winding number*, $N_{CS}$. The relation between the Chern-Simons number and the change in baryon

[2] Classically means with only perturbative calculations.

[3] Compare with classical electron current $\int_t \nabla \cdot \vec{J} = \Delta Q$, where $\vec{J}$ is the current, $t$ is time and $\Delta Q$ the change in charge.

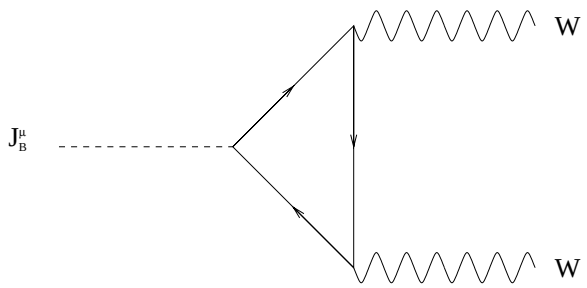


Figure 1.1: The triangle anomaly contributing to the baryon and lepton number currents, and thereby the violation of baryon and lepton number.

number can be expressed as:

$$\Delta B = \Delta N_{CS} = n_f[N_{CS}(t_1) - N_{CS}(t_0)], \tag{1.6}$$

where $n_f$ is the number of families and $N_{CS}(t)$ is the Chern-Simons (winding) number at time $t$. Hence, when the Chern-Simons number is changed by one, nine quarks, (three color states for each generation) and three leptons are created, giving $\Delta B = 3$ and $\Delta L = 3$. This change in Chern-Simons number is vehicled by either a *sphaleron* process or an *instanton*. Without pretending to know the details, I give the basic procedure as follows.

The electroweak potential can be sketched as in figure 1.2. There are several different vacua, like in the case of the pendulum, and the different vacua have different Chern-Simons number (like $n$ in the case of the pendulum). A transition between different vacua (and therefore different Chern-Simons number and hence a change in baryon number) can be obtained in two different ways. First, a tunneling event may occur, which is called an instanton. The probability of tunneling depends on the thermal energy, i.e., how "thick" the potential barrier between different Chern-Simons numbers is. Second, if the (thermal) energy is high enough, it is possible to pass above the potential walls separating the different Chern-Simons numbers (and different vacua). The solution at the highest point of the potential is called a sphaleron, but also a transition that *passes* over this point is called a sphaleron (or a sphaleron process). These two processes will be outlined in the following sections.[4]

[4]Nonlinear coherent structures such as kinks, solitons, sphalerons, vortices, and instantons arise in the study of a variety of interesting and important physical situations such as baryon number violation, properties of materials, optical communications, dynamics of phase transitions, and the physics of the early universe.

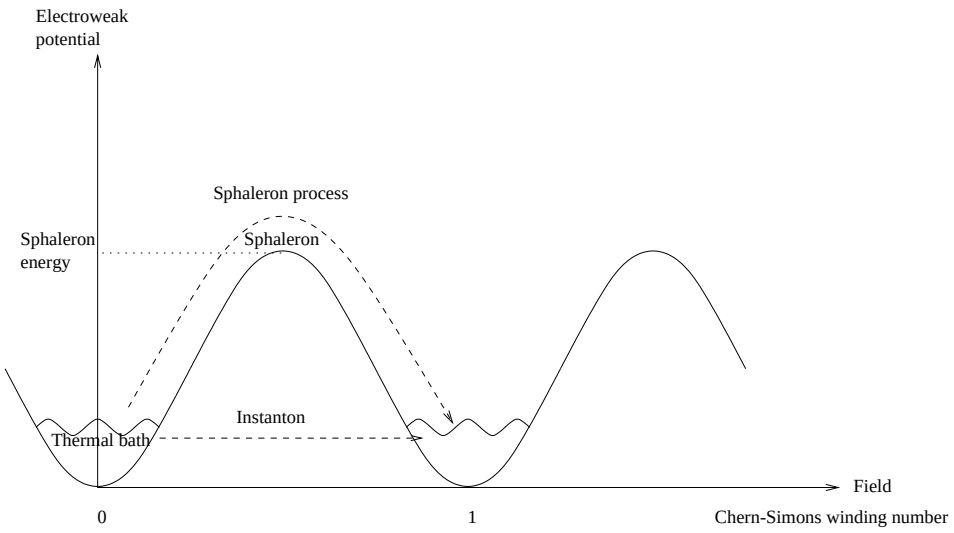


Figure 1.2: Sketch of electroweak potential with minima, Chern-Simons number, sphaleron and instanton.

### Sphalerons

Mathematically, a sphaleron is a special type of solution to a partial differential equation. It is a saddle-point solution to the equations of motion with a single negative eigenvalue.

It corresponds physically to the solution where the energy of the state is equal to that of the highest point of the (periodic) potential. For the electroweak potential, the energy of the spahleron can be calculated [12] to be

$$E_{sph}(T \approx 0) \approx 10 \text{ TeV}. \tag{1.7}$$

The result is only an approximation, but it still gives an idea of the order of magnitude of the sphaleron energy.

Note that the energy of the sphaleron actually depends on the temperature. The sphaleron energy decreases with increasing temperature, which means that when the temperature approaches the electroweak phase transition temperature $\sim 100$ GeV, the sphaleron energy is believed to discontinuously go to zero.

The rate per volume of baryon number violating effects can be approximated to be

$$\Gamma(T) \propto e^{-E_{sph}(T)/T} \tag{1.8}$$

for a certain regime [4] (probably) below the electroweak phase transition. This is the same type of transition rate formula as for the pendulum, and we expect that near the critical temperature the exponential suppression factor will take effect [13] (when decreasing the temperature).

As can be seen in the previous formula, the sphaleron processes will work against the production of a baryon-antibaryon asymmetry. In the scenario above, these sphaleron processes can be seen as the reason for the necessity of a thermodynamic non-equilibrium because the sphalerons vehicle the change in baryon number.

**Instantons**

Instantons are, like sphalerons, special types of solutions to partial differential equations. Intuitively, they can be described as an energy configuration in space-time. Physically, they describe the tunneling between different Chern-Simons numbers/vacua. The tunneling rate betweeen different Chern-Simons numbers can be calculated to be

$$\Gamma \propto e^{-S_E}, \tag{1.9}$$

where $S_E$ is the Euclidian action obtained from the Minkowski-space action by a Wick rotation $t \to -it \equiv \tau$. The tunneling rate at zero temperature can be calculated [4] to be

$$\Gamma(T = 0) \sim 10^{-170}. \tag{1.10}$$

Thus, in our everyday life, instanton processes will play a very insignificant role, and baryon number is virually conserved.

### 1.2.4 Charge and Charge-Parity Violation

In the previous section a rather detailed study of the baryon number violation has been done because it is closely related to the subject of this report, the hypercharge axion. As for the $CP$ violation, it has nothing to do with the axion, and only some brief remarks will be made.

Even though $C$ and $CP$ symmetries are known to be broken in the standard model, this source of $CP$ violation is far too small to produce the observed asymmetry between matter and antimatter.

In the minimal supersymmetric standard model (MSSM) $CP$ violation can be enhanced by including a second Higgs doublet or by higher dimension operators, but this subject is too vast to be treated in this report. For a

resumé of these effects, see [4]. This enhancement of the $CP$ violation could be strong enough to produce the present dominance of matter over antimatter.

## 1.3 The Axion

The indroduction of the hypercharge axion has two objectives. First, it explains the baryon number violation that gives rise to the matter-antimatter asymmetry in the universe. Second, it explains the existence of large-scale magnetic fields in diffuse astrophysical plasmas. The first Sakharov condition is the principal subject of this study of the axion. The second Sakharov condition, the presence of $C$ and $CP$ violation is expected to be explained elsewhere and the third Sakharov condition is supposed to be fulfilled by a strong first-order electroweak phase transition.[5]

The basic idea of the procedure from axion to baryon number violation is the following: The hypercharge axion couples to the hypermagnetic field, amplifying it to the extent that it gives sufficient baryon number violation to account for the matter-antimatter asymmetry.

This section covers the theoretical background and properties of the hypercharge axion.

### 1.3.1 Amplification of Hypermagnetic Fields

In the universe today, we observe mysterious large-scale magnetic fields. These could originate from hypermagnetic fields that existed before the electroweak phase transition. The hypermagnetic fields are thought to behave basically like the ordinary electromagnetic fields, obeying Maxwell's equations. With some different compositions there still exists two parts, one weak ($\mathrm{SU}(2)_L$) and one hyperelectromagnetic ($\mathrm{U}(1)_Y$).

The part of the baryon number violating term, which is important for the hypercharge axion, is expressed as

$$\partial_\mu J_B^\mu \propto Y_{\mu\nu}\tilde{Y}^{\mu\nu} \propto \vec{H}_Y \cdot \vec{E}_Y \tag{1.11}$$

because the hypercharge axion couples to the hyper(electro)magnetic fields, $H_Y$ and $E_Y$. In the equation, $Y_{\mu\nu}$ is the hypermagnetic field strength and $\tilde{Y}_{\mu\nu} = \epsilon_{\mu\nu\alpha\beta}Y^{\alpha\beta}$ is its dual ($\epsilon_{\mu\nu\alpha\beta}$ is the permutation symbol, defined in appendix B.)

[5] According to [16] long-range uniform magnetic fields could strengthen the electroweak phase transition to the point that the baryon number asymmetry could survive.

Normally, this source of baryon number violation is ignored because vacuum is supposed in the initial as well as in the final state.[6] However, in the theory of the hypercharge axion, we suppose that a hypermagnetic field exists before the electroweak phase transition. Where it comes from would be the issue of another study, but according to [15] there "are neither compelling theoretical arguments nor motivated phenomenological constraints which could exclude the existence of magnetic fields prior to the nucleosynthesis epoch." The same article also gives the ratio for the baryon-to-entropy ratio $\delta(n_B/s)$ due to the existence of the hyperelectromagnetic fields. The formula depends on space, time and hypermagnetic field strength.

In [16] it is shown that the existence of a hypercharge axion introduces a new term in the Maxwell equations, which is a coupling between the hypercharge axion field $X$ and the hypermagnetic field $B_Y$. The solution of the Maxwell's equations can be decomposed in Fourier modes with different frequencies. The equation of motion for the hypercharge axion can be solved and the solution are periodic oscillations or rolling around the minimum of its potential.

Depending on the frequency of the axion oscillation/rolling, it will couple to (=come to resonance with) different Fourier modes. More specifically there will be a certain mode that will be maximally amplified, while the nearby modes are amplified somewhat less. The amplification is exponential and can achieve values of $10^{12}$ or larger only after a few cycles. Such high hypermagnetic fields can lead to enough baryon asymmetry generation through equation (1.11). In order to preserve the baryon asymmetry, the oscillation or rolling should take place just before or during the phase transition to avoid diffusion of the magnetic modes, which erases the field, and thus the conditions for baryon number violation. In the scenario of a rolling hypercharge axion, the amplification will affect very long wavelength modes. These modes do not diffuse as quickly as higher wavelength modes. This means that the resonance does not have to occur at the moment of the electroweak phase transition, but could occur somewhat earlier.

### 1.3.2 The Lagrangian

The Lagrangian density describing hyperelectromagnetic fields coupled to the heavy pseudoscalar axion $X$ in the resistive approximation [16] of the

[6] Even when vacuum is supposed in the initial as well as the final state the weak part will still give rise to a baryon number changing current [4].

highly conducting electroweak plasma is:

$$\begin{aligned} L = \quad & \sqrt{-g}\left(\tfrac{1}{2}\nabla_\mu X \nabla^\mu X - V(X) - \tfrac{1}{4}Y^{\mu\nu}Y_{\mu\nu} - J_\mu Y^\mu - \tfrac{\lambda}{4}XY^{\mu\nu}\tilde{Y}_{\mu\nu}\right) \\ & -\mu\epsilon_{ijk}Y^{ij}Y^k, \end{aligned} \tag{1.12}$$

where $Y_{\mu\nu}$ is the hypercharge field strength, $Y^k$ is the hypercharge photon, $g = \det(g_{\mu\nu})$ is the determinant of the metric tensor, $\lambda \sim M^{-1}$ is a scaling constant, $\nabla_\mu$ is the covariant derivative, $V(X)$ is the axion potential and $J_\mu$ is the Ohmic current. The last term $\mu\ldots$ represents the possibility that a fermionic chemical potential survives the unbroken phase of the electroweak plasma. Finally, $\epsilon^{ijk}$ is the permutation symbol, which is 1 for all even permutations of $\epsilon^{123}$, -1 for all odd permutations and 0 for all other values of the indices.

An explanation of the different terms in the Lagrangian can now be appropriate.

$\frac{1}{2}\nabla_\mu X \nabla^\mu X$ is the good old dynamic term, correponding to $\frac{mv^2}{2}$ in classical mechanics.

$V(X)$ is the potential of the hypercharge axion, which can be approximated [16] to be $\frac{1}{2}M_Y^2X^2$, a harmonic oscillator potential. $M_Y$ is a mass-scale, see below.

$\frac{1}{4}Y^{\mu\nu}Y_{\mu\nu}$ is the hyperelectromagnetic energy, which is proportional to $\vec{E}_Y \cdot \vec{H}_Y$ ($\vec{E}$ and $\vec{H}$ being, respectively, the hyperelectric and hypermagnetic field).

$J_\mu Y^\mu$ is the ordinary current of electric charge.

$-\frac{\lambda}{4}XY^{\mu\nu}\tilde{Y}_{\mu\nu}$ is the interaction between the hypercharge axion and the hyperelectromagnetic field, see below.

### 1.3.3 Couplings

The part of the Lagrangian that is of interest for the detection in accelerators is the interaction between the hypercharge axion[7] $X$ and the hyperelectro-

[7] In fact, it is this coupling that has given the name to the hypercharge axion. The coupling is the same as for the quantum chromodynamics axion, which was proposed as a possible explanation for the non-existence of a strong equivalent to the weak $CP$ violating term. For more information, see, e.g., [14].

magnetic field $Y_{\mu\nu}$:

$$L = \frac{1}{8M_Y} X Y_{\mu\nu} \tilde{Y}^{\mu\nu}, \tag{1.13}$$

where $\tilde{Y}^{\mu\nu} = \epsilon^{\alpha\beta\mu\nu} Y_{\alpha\beta}$ is the dual of the hyperelectromagnetic field, $M_Y = \frac{1}{2\lambda}$ is the mass-scale of the hypercharge axion, which in principle could be anything that is much larger than the mass of the axion, $m_X$. We can obtain the Lagrangian in terms of $Z^0$s and photons if we decompose the hypercharge fields into the $Z^0$, and the photon,

$$\begin{aligned} Y_{\mu\nu} &= \partial_\mu Y_\nu - \partial_\nu Y_\mu, \\ Y_\mu &= A_\mu \cos\theta_W - Z_\mu \sin\theta_W, \end{aligned} \tag{1.14}$$

where $A_\mu$ is the photon field, $Z_\mu$ is the $Z^0$, and $\theta_W$ is the weak mixing angle. We obtain

$$\begin{aligned} L = \tfrac{X\epsilon^{\mu\nu\rho\sigma}}{8M_Y}[ \quad & a(\partial_\mu A_\nu \partial_\rho A_\sigma) + b(\partial_\mu Z_\nu \partial_\rho Z_\sigma) \\ & -c(\partial_\mu A_\nu \partial_\rho Z_\sigma) - c(\partial_\mu Z_\nu \partial_\rho A_\sigma)], \end{aligned} \tag{1.15}$$

where $a = \cos^2\theta_W$, $b = \sin^2\theta_W$ and $c = \sin\theta_W \cos\theta_W$. Here we can clearly see the interactions and their coupling constants. In the first term we see the $X \to \gamma\gamma$ coupling, in the second the $X \to Z^0 Z^0$ coupling, and in the third and fourth the $X \to Z^0\gamma$ coupling.

### 1.3.4 Branching Ratios

The *branching ratios* of the processes can be obtained from the matrix elements of the Lagrangian:

$$\begin{aligned} \Gamma_{X\to\gamma\gamma} &= \tfrac{1}{32\pi M_Y^2} \cos^4\theta_W \left[m_X^3\right] \\ \Gamma_{X\to Z^0\gamma} &= \tfrac{4}{32\pi M_Y^2} \cos^2\theta_W \sin^2\theta_W \left[\tfrac{(m_X^2 - m_Z^2)^3}{M_X^3}\right] \\ \Gamma_{X\to Z^0 Z^0} &= \tfrac{1}{32\pi M_Y} \sin^4\theta_W \left[(m_X^2 - 4M_Z^2)^{3/2}\right], \end{aligned} \tag{1.16}$$

where $\theta_W$ is the weak mixing angle, $m_X$ is the mass of the axion, $M_Y$ is the mass-scale, and $M_Z$ is the $Z^0$ mass.

We note that the squared coupling constants from equation (1.15) are here as well as the mass-scale squared. The factor 4 for $X \to Z^0\gamma$ comes from the two last terms in equation (1.15) which are identical.

The total width for $m_X \sim 1$ TeV, $M_Y \sim 1$ TeV is about 1 GeV.

### 1.3.5 Candidates for the Hypercharge Axion in Extensions of the Standard Model

Brustein and Oaknin treat this subject in [17]. There are several pseudoscalars in different extensions of the standard model that couple to the hypercharge as proposed in equation (1.13). In order to drive baryogenesis, a condition on the rolling/oscillating time must be fulfilled [17].

One candidate would be the heavy Higgs pseudoscalar in the supersymmetric standard model, but this coupling is shown to vanish in the symmetric phase of the electroweak theory. Other possible candidates, like the pseudoscalar component of sneutrinos, do not couple to the hypercharge.

In string theory there are several possible pseudoscalars but the condition mentioned above turns out to be difficult to fulfil. Besides, the coupling to the hypercharge generally happens at temperatures much higher than the electroweak phase transition. In summary, it is possible that the hypercharge axion could be described by string theory, but the conditions are rather severe.

# Chapter 2

# Phenomenology of the Hypercharge Axion

This chapter discusses the experimental aspects and the phenomenology of the hypercharge axion. It describes the signatures and background for the detection of such a particle in the ATLAS detector at the future large hadron collider (LHC) at CERN.

First the detector is presented briefly to situate the project in the context. Second, the characteristics of axion decay are discussed as well as the process that is the subject of this thesis

$$q + \bar{q} \rightarrow q + \bar{q} + \gamma + \gamma \rightarrow q + \bar{q} + X \tag{2.1}$$

with subsequent decay of the axion to photons and $Z^0$s. Third, the approximations are presented. The interactions are simulated with a Monte Carlo program (PYTHIA) and the detector with ATLFAST. The semi-classical Weizsäcker-Williams approximation is made for the emission of photons from the primary partons. Fourth, the general backgrounds ($\gamma, Z^0$ and jets) are discussed with their characteristics and their effect on our signals. Fifth, the different processes that originate from the existence of the axion are presented. There are several, but only a few can be detected in ATLAS.

## 2.1 The Detector

### 2.1.1 Large Hadron Collider

The large hadron collider (LHC) is a particle accelerator that is built at CERN (European laboratory for particle physics) and will be ready for experiment in 2005. The accelerator will bring protons and, later, ions into

head-on collisions with higher energies than ever before. These high energies will allow physicists to probe deeper into the structure and the fundamental properties of matter and energy. The elevated energy will allow new types of particles to be created, detected and measured, but they will not be easy to detect.

Along with the new, interesting physics there will be huge amount of background, or noise, coming from other processes that are already known. The principal reason behind this background is the fact that a proton is made of three quarks, which makes the collision a six-body problem. It is not easy to calculate and predict theoretically, nor to accurately detect all outgoing particles.

LHC will be able to produce three basic types of reactions. First, it can collide proton beams, each proton having an energy of 7 TeV, for a total of 14 TeV in the interaction. This will be the main type of collision at LHC and the luminosity[1] will reach $10^{34}$ $\mathrm{cm}^{-2}\mathrm{s}^{-1}$, which is about 100 times higher than that of current colliders. Second, heavy ions, like lead, can be collided with a total energy of 1250 TeV in the collision, about 30 times higher than that of the Relativistic Heavy Ion Collider (RHIC) at the Brookhaven Laboratory in the US. Third, on long term it is planned to combine LEP and LHC. Electron-proton collisions can be obtained with total energies of $\sim 1.5$ TeV, about five times higher than HERA at the DESY laboratory in Hamburg.

### 2.1.2 The ATLAS detector

The ATLAS (A Toroidal LHC ApparatuS) detector is one of the detectors on LHC. It is immense (like a five-story building) and is hermetically closed. The parts of ATLAS that are relevant for this research are:

**Inner tracker** - measures the momentum of each charged particle. The inner tracker is inside a solenoidal magnet of 2 Tesla, bending the charged particle tracks and allowing measurement of their momenta.

**Calorimeter** - measures the energies carried by the particles. There is one electromagnetic calorimeter and one hadronic calorimeter. The calorimeters are thick enough to let through only $10^{-7}$ percent of the entering particles.

[1] Luminosity $\mathcal{L}$, is directly proportional to the number of particles in each bunch and to the bunch-crossing frequency, and inversely proportional to the area of the bunches at the collision point.

**Muon spectrometer** - identifies and measures muons. The muons interact so feebly with matter that most of them pass the calorimeter without stopping and without causing a shower of particles. The muon spectrometer consists of chambers to measure their track. A strong toroidal magnetic field is present to measure their momenta.

There is also a trigger system that selects hundreds of interesting events from thousands of millions of others and a data aquisition and filtering system to further classify and distinguish each event (collision every 25 ns).

Obviously, the detector has a limited resolution, which, e.g., means that a quark will be observed as a shower, a jet. Also, photons with low transverse momentum will not be detected, and particles have to be separated by a certain angle to be identified as different particles.

## 2.2 Characteristics of the Hypercharge Axion

### 2.2.1 Interactions

What is interesting for us is the interaction the axion would have with matter. Let us investigate the interaction of the pseudoscalar axion field $X$ with the hypercharge field strength $Y_{\mu\nu}$. This is described by the Lagrangian

$$L = \frac{1}{8M_Y} X Y_{\mu\nu} \tilde{Y}^{\mu\nu}, \tag{2.2}$$

where $M_Y$ is a scale factor with the dimension of energy, and $\tilde{Y}^{\mu\nu} = \epsilon^{\alpha\beta\mu\nu} Y_{\alpha\beta}$ is the dual of the hypercharge field strength. This is the Lagrangian proposed by Brustein and Oaknin [3]. Obviously there are several other interactions in the system, including potentials and self-interactions, but these do not influence the results of this section. For a more detailed discussion, see section 1.3. We will take $M_Y$ as a free parameter and determine for which values of $M_Y$, and for which masses of the axion $m_X$, it will be possible to discover the axion in ATLAS . The actual values of $M_Y$ and $m_X$ depend on the theory invoked to make the connection between the matter-antimatter problem and the hypercharge axion, see section 1.3.5.

The hypercharge field-strength consists basically of $Z^0$s and photons, which means that the interaction will be between the axion and either two photons, two $Z^0$s or one $Z^0$ and one photon. Hence, to identify the hypercharge axion in the detector, we will look for these three types of decay products. With the particles coming out from the collision, we will look

for photons and[2] $Z^0$s and reconstruct the invariant mass[3] of these particles. This mass should be equal to the mass of the axion, and with a lot of events it should be recognizable above the background.

As the hypercharge axion is expected to be rather heavy, its decay products will often have a high transverse momentum. Most other particles will more or less follow the direction of the beam due to the high momentum in the beam direction. Hence, another characteristic of the axion will be off-axis photons and $Z^0$s.

### 2.2.2 The Event

Brustein and Oaknin [3] proposed the channel $f + \bar{f} \to Z^*/\gamma^* \to Z/\gamma X$ for detection of the hypercharge axion $X$. However, the cross section for this process is rather low and another possibility to detect the axion will be investigated here to complement their work.

We will study emission of two photons (one from each proton) colliding to give the axion. In the proton, generally only one of the quarks (an up or a down quark) or a gluon will interact in the collision with another quark or gluon from the other proton. The event that is the subject of this research can therefore be written as (figure 2.1)

$$q + \bar{q} \to q + \bar{q} + \gamma + \gamma \to q + \bar{q} + X, \tag{2.3}$$

where the axion can disintegrate as

$$\begin{aligned} X \quad &\to \gamma + \gamma \\ &\to Z^0 + \gamma \\ &\to Z^0 + Z^0. \end{aligned} \tag{2.4}$$

We can make a rough estimate of the number of events for a certain mass of the axion, say 1 TeV. The number of events is, by definition, the product of luminosity, time and cross section:

$$N_{ev} = \mathcal{L} \times t \times \sigma \sim 10^{28}\ \mathrm{cm}^{-2}\mathrm{s}^{-1} \times 10^{7}\ \mathrm{s} \times 150\ \mathrm{pb} \times 10^{-24}\ \mathrm{b/cm}^2 \approx 15. \tag{2.5}$$

[2] In fact, we look for the decay products of the $Z^0$s, see below.

[3] The invariant mass $M$ is defined as

$$M^2 = \left(\sum_i E_i\right)^2 - \left|\left|\sum_i \vec{p}_i\right|\right|^2,$$

where $E_i$ and $\vec{p}_i$ are, respectively, the energy and the momentum of particle $i$, and $||\vec{v}||^2 = v_x^2 + v_y^2 + v_z^2$ is the squared norm of the vector $\vec{v}$.

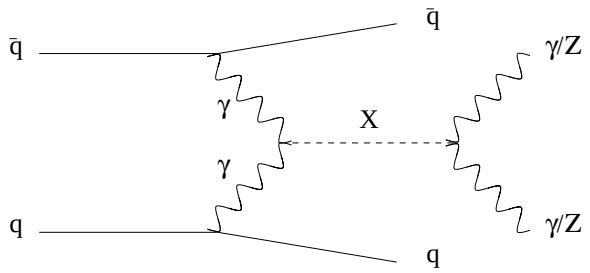


Figure 2.1: The event that is the object of this study. Two quarks within the proton emit two photons, which collide and produce the axion, which disintegrates to photons and/or $Z^0$s.

Here the $\gamma\gamma \to X$ cross-section, $\sigma$, at the resonance is taken from [3] with the mass-scale $M_Y = 1$ TeV, and where the luminosity $\mathcal{L}$ is extrapolated from the graph in [18] and integrated over the resonance width of the axion (about 1 GeV). This is the luminosity for the production of two photons with invariant mass $\sim 1$ TeV during LHC operation at low luminosity. It is calculated assuming coherent emission from a proton. In fact, it can be much higher if the photons are emitted from quarks and the proton is allowed to disintegrate. The time $t$ is taken to be one year of running, or $10^7$ s, and $10^{-24}$ b/cm$^2$ is a rough conversion factor from cm$^{-2}$ to barn. This is detectable, though the signal will be rather feeble. This means that we have to be more careful with the background. To increase the signal we will assume that we run during three years of high luminosity at LHC, giving ten times as many events:

$$N_{ev} \sim 150. \tag{2.6}$$

The forward jets could in principle serve as a signature for the process, but the enormous jet background in the LHC will completely destroy this possibility. This jet background (also called QCD background) comes from interactions between quarks. These interactions produce outgoing quarks that will give showers of particles in the decay process. These showers are detected in ATLAS and are called jets. Because LHC works with proton collision (i.e., strong interactions) at extremely high energies there will also be a large number of jets, in the background.

We can also use the fact that the decay products of the axion (the $Z^0$s and photons) are produced virtually *back-to-back* in the transverse plane, i.e., the angle between the two particles in the transverse plane is 180 degrees. The reason for this is that the two photons producing the axion have

almost zero transverse momentum (in comparison with their longitudinal momentum) which comes from the fact that the quarks in the proton have very low transverse momenta.

In summary, the characteristic of the axion are decay products $X \rightarrow \gamma\gamma$, $Z^0Z^0$ or $Z^0\gamma$ with an invariant mass producing a bump, emitted back-to-back and with high $p_T$.

## 2.3 Approximations

### 2.3.1 Monte Carlo Simulation

The events have been generated in PYTHIA [19] which is a Monte-Carlo simulation program for particle interactions. To simulate the detector effects with its limits in resolution and acceptance ATLFAST has been used. This means, among other things, that photons with $p_T < 60$ GeV will not be detected and that photons which are too close to the beam axis will be mistaken for jets.

The generation of the matrix elements to calculate the interactions have been provided by Gilles Couture. He has used the Weizsäcker-Williams approximation for the emission of the two photons and the parton distribution functions from [21], mostly Appendix A.

### 2.3.2 Weizsäcker-Williams Approximation

For the interaction between the two quarks, the *Weizsäcker-Williams approximation* (also called equivalent photon approximation or almost-real-photon approximation) has been made. In principle the electromagnetic field of the charged particle is treated as (almost) real photons. These can interact with the almost real photons from the other charged particle. This approximation is only valid when the transverse momentum of the charged particle is virtually zero, and when they have ultra-relativistic speeds. This should be fairly well accomplished in our scheme, as the charged particle is a quark, and the quarks inside a proton have very little transverse momentum and the speed is only a small fraction from that of light. Another consequence of this approximation is that the protons are supposed to split and produce fragments in the forward direction.

There does not exist any good theoretical description of $\gamma\gamma$ processes from proton-proton collisions. However, the Weizsäcker-Williams approximation suffices well.

## 2.4 Background

The background consists of all processes that give the same type of signal as the interesting event. An everyday example would be to weigh different animals, trying to distinguish them *only* by their weight. Suppose that we look for the elephant (the axion). We would have an enormous number of light animals, like insects, indistinguishable from each other, (loosely corresponding to the QCD background, see below). As the size goes up, fewer and fewer animals are heavy enough. Eventually, we might see a bump for humans around 70 kg, and around 5 tons we find the indian elephant bump. However, there are other animals that could be this heavy, rhinoceros and whales for example, though it would be rare. This is the background.

This section is dedicated to the different backgrounds for the axion. First, the interesting processes will be presented so that we know what backgrounds to consider. In summary, these backgrounds are processes producing photons and $Z^0$s each of which will be discussed separately. A brief discussion of the jets is also included.

In the calculation of the backgrounds for the different processes, the contribution of the Higgs boson is excluded. This is done because the Higgs boson has an unknown mass, which makes it difficult to estimate the background it could produce for the process. In fact, we do not even know that it exists. If it exists as expected with a mass of 115 GeV, its contribution would be negligible, because the branching ratios of $H^0$ to photons and $Z^0$s are very small [22].

### 2.4.1 Decay Channels

The possible decay channels of the axion are (with branching ratios[4] over the arrows):

$$\begin{array}{lllll} X & \xrightarrow{44\%} & \gamma+\gamma & & \\ & \xrightarrow{52\%} & \gamma+Z^0 & \xrightarrow{6\%} & \gamma+l+\bar{l} \\ & & & \xrightarrow{70\%} & \gamma+jet+jet \\ & \xrightarrow{4\%} & Z^0+Z^0 & \xrightarrow{0.36\%} & l+\bar{l}+l+\bar{l} \\ & & & \xrightarrow{3.6\%} & l+\bar{l}+jet+jet \\ & & & \xrightarrow{36\%} & jet+jet+jet+jet, \end{array} \tag{2.7}$$

[4]The branching ratios of the axion depend on its mass, but this dependence is very weak (see section 1.3.4). In the range $500 < m_X < 5000$ GeV the difference is less than a few tenth of percentage.

where we have used the fact [20] that the $Z^0$ decays to two specific leptons 3 percent of the time, to two quarks (jets) 70 percent of the time and to neutrinos the rest of the time. The $\tau$ is more difficult to detect at the LHC and is not considered here, leaving the electron and muon, for a total of 6 percent detectable lepton decays.

As we can see, our primal branchings will be:

$$\begin{array}{ll} X & \rightarrow \gamma + \gamma \\ X & \rightarrow \gamma + Z^0 \rightarrow \gamma + l + \bar{l} \end{array} \tag{2.8}$$

because $X \rightarrow Z^0 + Z^0$ is rare and $X \rightarrow \gamma + jet + jet$ is very polluted by the QCD background. A more detailed discussion follows below in section 2.5. Before discussing this further some general backgrounds will be described.

### 2.4.2 $\gamma$ Background

We can have photon emission at different stages in the calculations. First, in *initial and final state radiation*. Second, in specific processes giving photons as end-products. Third, a jet can be taken to be a photon in the detector.

#### Initial and Final State Radiation

Initial and final state radiation are decays of particles that occur before and/or after the event. Examples of initial/final state radiation are $q \rightarrow q\gamma$ and $q \rightarrow qg$.

#### Photon Processes

The principal processes that give rise to photon production in LHC are

$$\begin{array}{lcllcl} f\bar{f} & \rightarrow & \gamma/Z^0 & fg & \rightarrow & f + \gamma \\ f\bar{f} & \rightarrow & g + \gamma & gg & \rightarrow & g + \gamma \\ f\bar{f} & \rightarrow & \gamma + \gamma & gg & \rightarrow & \gamma + \gamma \\ f\bar{f} & \rightarrow & \gamma + Z^0, & & & \end{array} \tag{2.9}$$

where the fermion $f$ is a quark in our case and $g$ is the gluon. The processes $f\bar{f} \rightarrow g + \gamma$ and $gg \rightarrow g + \gamma$ have a high cross-section, but on the other hand they do not correspond to the exact final state of any of our processes. As for the other processes, they all have a very small cross-section, leaving us with a fairly small photon background.

Another process that could be expected to contribute is $gg \rightarrow \gamma Z^0$. The contribution would be to the background of $X \rightarrow Z^0\gamma$, but it is not included in PYTHIA and will not be included in our study.

**Fake Photons**

The resolution of the photons is rather good, but in some rare cases (approximately 1 time in 3000) a jet can be mistaken for a photon [23]. When the signal is strong, this is not a problem. However, when the signal is weak, this "fake" photon background could also be significant.

### 2.4.3 $Z^0$ Background

As two of the three branchings of the axion produce $Z^0$s it is important to see which other processes give $Z^0$s. A $Z^0$ can be produced in several different ways:

$$\begin{array}{llll} f+\bar{f} & \rightarrow & \gamma/Z^0 & f+g \rightarrow f+Z^0 \\ f+\bar{f} & \rightarrow & g+Z^0 & (Z^0Z^0 \rightarrow Z^0+Z^0) \\ f+\bar{f} & \rightarrow & \gamma+Z^0 & (W^+W^- \rightarrow Z^0+Z^0) \\ f+\bar{f} & \rightarrow & Z^0+Z^0 & \end{array} \tag{2.10}$$

Among these processes $f+\bar{f} \rightarrow g+Z^0$ and $f+g \rightarrow f+Z^0$ have high cross-section but do not directly lead to one of the final states of the axion decay either. This means that the missing photon will have to come from initital and/or final state radiation, as described in section 2.4.2. Fortunately, a high-$p_T$ photon from these sources is very improbable, diminishing the importance of these background processes.

For $Z^0Z^0 \rightarrow Z^0+Z^0$ and $W^+W^- \rightarrow Z^0+Z^0$, the cross-sections are extremely small, making it rather safe to exclude them from the calculations (see equation 3.2).

### 2.4.4 Jet Background

The QCD processes that have been generated are

$$\begin{array}{llll} q_iq_j & \rightarrow & q_iq_j & q_i\bar{q}_i \rightarrow q_k\bar{q}_k \\ q_i\bar{q}_i & \rightarrow & gg & q_ig \rightarrow q_ig \\ gg & \rightarrow & q_k\bar{q}_k & gg \rightarrow gg, \end{array} \tag{2.11}$$

where the evolution and showers come from initial and final state radiation as described in section 2.4.2.

In LHC there will always be an enormous background from jets due to the high energy and luminosity of the beam. This means that it will be very noisy to try to detect events with jets as final states. If the mass of the axion is relatively high, the criterion of high-$p_T$ decay products can be used

to reduce the background significantly. Normally, the produced jets will follow the beam direction because the quarks have relatively low-$p_T$ in the protons. However, the problem with a heavy axion is that its cross section for axion production decreases with increasing mass. This means that even with a low background, the cross-section for axion production might be too low to allow detection.

We know that the signal studied should have two and only two jets. However, since we have used the Weizsäcker-Williams approximation we cannot exploit this characteristic to apply cuts on the number and angle of the jets.

## 2.5 Processes

As can be seen from the branching ratios in the previous section and the estimate of number of events, equation (2.6), there will be almost no events with production of the $Z^0$s. Furthermore, LHC has a huge QCD background (jets) making it a difficult task to discern $Z^0 \to jet+jet$. This leaves us with two principal processes, $X \to \gamma+\gamma$ and $X \to \gamma+Z^0 \to \gamma+l+l$. These will be described in more detail below, while the others will be treated briefly in a separate subsection.

### 2.5.1 Process $X \to \gamma + \gamma$

This process should be very clean. Photons are rather easy to detect and their energies and momenta can be determined with good precision. Most of the noninteresting events (background) will be possible to sort out because the photons are produced back-to-back in the transverse plane, generally with high transverse momentum.

The background processes that should be important are

$$\begin{array}{l} f\bar{f} \to \gamma\gamma \\ gg \to \gamma\gamma, \end{array} \tag{2.12}$$

along with the other processes in equation (2.9) with initial and final state radiation to produce the other photon.

The $\gamma\gamma$ decay channel will be our principal source of events that hints at the existence of the axion because of its high branching ratio (44 percent) and the fact that photons are easily identified and (normally) do not decay.

### 2.5.2 Process $X \to \gamma + Z^0 \to \gamma + \bar{l} + l$

This process will also be very clean, but unfortunately also very rare. The total branching ratio for this process will be 3.1 percent and with the estimated total number of events equation (2.6) this leaves about five events that will be produced during three years of high luminosity at the LHC. When we add the limits of the detector, along with the condition that three particles should be detected ($\gamma\bar{l}l$), the number of observed events should be very small, at least for $m_X \sim 1000$ GeV.

The background processes that should be important are

$$\begin{aligned} f\bar{f} &\to \gamma/Z^0 \\ f\bar{f} &\to \gamma + Z^0, \end{aligned} \tag{2.13}$$

and the other processes in equation (2.10) with initial and final state radiation providing the photon.

### 2.5.3 Other processes

**Process** $X \to \gamma + Z^0 \to \gamma + jet + jet$

The process $X \to \gamma + Z^0 \to \gamma + jet + jet$ has a fairly high branching ratio (36 percent), which gives a good number of such events. However, as mentioned before, the fact that the jets have to be used to reconstruct the invariant mass of the $Z^0$ is very unfortunate. Even with the back-to-back criterion and the high-$p_T$ criterion, the QCD background (see section 2.4.4) is overwhelming and effectively drowns the signal.

**Process** $X \to Z^0 + Z^0 \to l + l + l + l$

The process $X \to Z^0 + Z^0 \to l + l + l + l$ should be very clean, but also very rare. Combining the low total branching ratio (0.0144 percent) with the difficulty for the detector to observe four distinct leptons leaves us without a single such event during three years of high luminosity at the LHC.

Still, the event will be very clean because each pair of leptons can be combined to produce the invariant mass of $Z^0$. The $Z^0$s then give the invariant mass of the axion and, in addition, they should be back-to-back, like in the case of $X \to \gamma\gamma$.

Possible background events come from $f\bar{f} \to Z^0 Z^0$.

**Process** $X \rightarrow Z^0 + Z^0 \rightarrow l + \bar{l} + jet + jet$

This process should be rather polluted because of the large QCD background that will give jets, and $Z^0$ emission that will give the leptons, as discussed in section 2.4.3. Furthermore, the signal in itself will be very weak (branching ratio 0.14 percent) and difficult to detect with its four particle final state.

An example of background is

$$t + \bar{t} \rightarrow bW^+ + \bar{b}W^- + \rightarrow jet + jet + l^+ + \nu + l^- + \bar{\nu}. \tag{2.14}$$

**Process** $X \rightarrow Z^0 + Z^0 \rightarrow jet + jet + jet + jet$

The process $X \rightarrow Z^0 + Z^0 \rightarrow jet + jet + jet + jet$ has only the back-to-back and high-$p_T$ criteria to differentiate it from the enormous QCD background. These criteria are far too weak to make the signal discernable above the background.

# Chapter 3

# Results and Analysis

As discussed in the previous chapter, the simulation of the processes and the backgrounds has been done in PYTHIA [19], with the axion interaction as an externally included process and with ATLFAST for simulation of the ATLAS detector.

This chapter consists of four parts: The simulation of the signal of the different decay channels, the simulation of the background, both together, and finally some conclusions. The simulation of the signal is done for different masses of the axion and gives us a hint of where a search could be fruitful. The signal will be stronger for lower masses, but the background will also be stronger. The analysis of the background will be done completely for $m_X \sim 1000$ GeV. This gives an indication of which background processes are significant. This is important to know because at lower energies we have to generate more events as the cross-section goes up. The backgrounds that are found to be important are simulated also for $m_X \sim 800$ GeV.

## 3.1 Signal

First of all we calculate the luminosity for different invariant masses of $\gamma\gamma$. The process is $q + \bar{q} \to q + \bar{q}\gamma\gamma$. These are the photons that will interact to produce the axion and consequently their invariant mass should be the invariant mass of the axion. When we assume a total luminosity of $10^{33}$ $\mathrm{cm}^2\mathrm{s}^{-1}$ we obtain the result shown in figure 3.1. Now, we calculate the cross-sections of the processes. With the cross-sections we calculate how many events we expect through

$$N_{ev} = \mathcal{L} \times t \times \sigma. \tag{3.1}$$

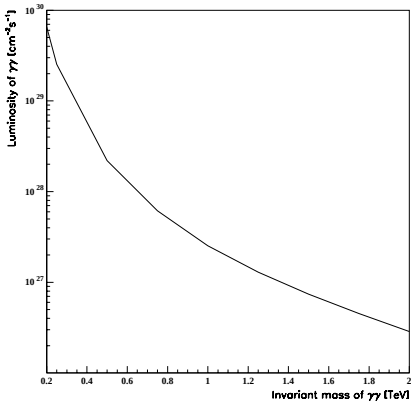


Figure 3.1: Luminosity of $\gamma\gamma$ production as a function of their invariant mass for a pp luminosity of $10^{33}$ cm$^{-2}$s$^{-1}$.

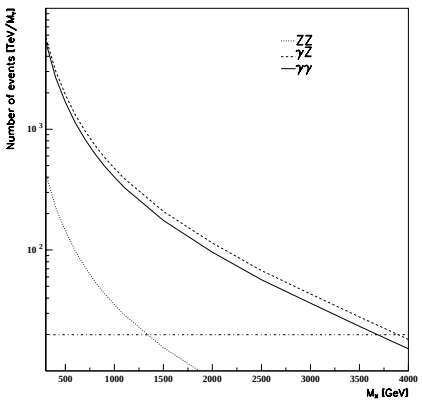


Figure 3.2: Number of events produced for the different processes for three years of high-luminosity LHC operation.

We will require at least ten events and we assume three years of high luminosity, which gives an integrated luminosity[1] of 300 fb$^{-1}$. The number of events will be measured in units of $(\frac{\text{TeV}}{M_Y})^2$. However, we lose more than half of the events in the ATLAS detector due to problems with resolution and the fact that the detection of photons is not possible at near forward angles. This means that we need at least $N_{ev} > 20$ to really detect the particle. Figure 3.2 shows the number of axions produced as a function of axion mass, $m_X$, for the different decay channels. We see that for an axion mass $m_X \sim 1000$ GeV the number of events is almost a factor ten higher than the one predicted from equation (2.6). The reason for this is that the photon emission is done directly from the quarks, and the proton is allowed to disintegrate (see explanation following equation (2.5)). Note that this is only a first estimate and that the background has to be considered too. This is done in the following section.

[1] Integrated luminosity is $\mathcal{L} \times t$.

## 3.2 Backgrounds

In this section we will discuss preselection cuts on the background, which means that we limit the kinematic phase space in order to decrease the cross-section. Otherwise we would have to generate an enormous amount of background. We also generate the complete backgrounds for $m_X \sim 1000$ GeV and the significant backgrounds for $m_X \sim 800$ GeV. The signal and the backgrounds are discussed together in the next section, 3.3.

### 3.2.1 Cuts

In order not to a have to generate an overwhelming number of background events we introduce preselection in the calculations. A preselection means that an event is rejected at an early state because it does not fulfil certain criteria. The cuts in our simulation have been made on the transverse momentum $p_T$ and the center-of-mass energy $\sqrt{\hat{s}}$ of the two partons participating in the reaction. As discussed in chapter 2 a characteristic of the axion is high-$p_T$ decay products, motivating a cut exclude $p_T < 300$ GeV which should be valid for $m_X > 700$ GeV. In order to even create something similar to the axion, the center-of-mass energy should be comparable to the mass of the axion. We have chosen to exclude $\sqrt{\hat{s}} < m_X - 100$ GeV.

To validate these cuts, the backgrounds have been simulated with lower cuts. With proper normalization[2] the two signals are then compared. In the region around $m_X$ the shape of the curves should be similar. An example is shown in figure 3.3.

These were preselection cuts, which act in the generation of events to reduce the cross-sections. In consequence of the 3$^{\text{rd}}$ characteristic of the axion we apply a third cut, but this can only be done after the generation of events. This is a cut on the angle in the transverse plane between the particles that could have been the decay products of the axion. How these particles are selected is discussed below. The cut on the angle is $3.0 < \phi < \pi$.

Obviously, all these cuts must also be applied on the signals themselves. This will reduce the signal, but even more so the background, which in principle should be randomly distributed.

#### Selection Criteria

The selectrion criteria for the different processes are:

[2]When two signals have different cross-sections they must be normalized. The normalization factor is $N = \frac{\sigma_1/N_1}{\sigma_2/N_2}$, where $N_i$ is the number of generated events for signal $i$.

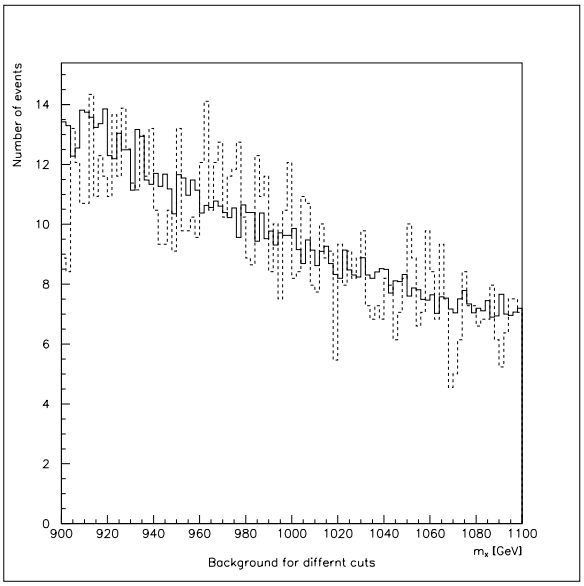


Figure 3.3: Comparison of reconstructed $m_{\gamma\gamma}$ from background $f\bar{f} \to \gamma + \gamma$, with preselection cuts, $\sqrt{\hat{s}} > 900$ (full histogram) and $\sqrt{\hat{s}} > 700$ (dashed histogram).

$X \to \gamma\gamma$ Select the two photons with highest transverse momentum and calculate their invariant mass.

$X \to Z^0\gamma \to \bar{l}l\gamma$ Select the two leptons with highest transverse momentum, calculate their invariant mass (should give the $Z^0$), select the photon with highest transverse momentum and calculate the invariant mass with the reconstructed $Z^0$.

$X \to Z^0\gamma \to jet + jet + \gamma$ Same as $Z^0 \to ll$ except that the leptons are replaced by the jets.

$X \to Z^0Z^0 \to \bar{l}l\bar{l}l$ Select the four leptons with highest transverse momentum, calculate the invariant masses between all the leptons, choose the pair that gives the mass closest to that of the $Z^0$. The other pair is supposed to give the other $Z^0$, and together the pairs give the mass of the "axion".

$X \to Z^0Z^0 \to \bar{l}l + jet + jet$ Same principle as for $Z^0Z^0 \to \bar{l}l\bar{l}l$.

$X \to Z^0Z^0 \to jet + jet + jet + jet$ Same principle as for $Z^0Z^0 \to \bar{l}l\bar{l}l$.

**QCD background** In some rare cases (about 1 in 3000) a jet can be mistaken for a photon and the selection process for this is to choose the photon and the jet with highest $p_T$ and calculate their invariant mass.

### 3.2.2 Complete Background for $m_X \sim 1$ TeV

As stated in the previous chapter, there are several different backgrounds that will affect the signal. The cross-sections are calculated with the two initial cuts, $p_T > 300$ GeV and $\sqrt{\hat{s}} > 900$ GeV. For three years of high luminosity at the LHC, the integrated luminosity is 300 fb$^{-1}$ and the number of expected events is calculated from this. The specific backgrounds that have been treated in more detail are:

| **Initial** | | **Final** | **Actual # of events** | **Simulated # of events** |
|---|---|---|---|---|
| $f\bar{f}$ | $\rightarrow$ | $\gamma/Z^0$ | 46200 | 59910 |
| $f\bar{f}$ | $\rightarrow$ | $g+\gamma$ | 202020 | 400000 |
| $f\bar{f}$ | $\rightarrow$ | $g+Z^0$ | 303300 | 400000 |
| $f\bar{f}$ | $\rightarrow$ | $\gamma+\gamma$ | 2276 | 10000 |
| $f\bar{f}$ | $\rightarrow$ | $\gamma+Z^0$ | 5193 | 10000 |
| $f\bar{f}$ | $\rightarrow$ | $Z^0+Z^0$ | 6732 | 34410 |
| $fg$ | $\rightarrow$ | $f+\gamma$ | 886500 | 400000 |
| $fg$ | $\rightarrow$ | $f+Z^0$ | 1261500 | 400000 |
| $Z^0Z^0$ | $\rightarrow$ | $Z^0+Z^0$ | 0 | 0 |
| $WW$ | $\rightarrow$ | $Z^0+Z^0$ | 3 | 0 |
| $gg$ | $\rightarrow$ | $\gamma+\gamma$ | 66 | 10000 |
| $gg$ | $\rightarrow$ | $g+\gamma$ | 57 | 10000 |
| $\gamma+jet$ | $\rightarrow$ | $\gamma\gamma$ | 564450 | 400000 |

(3.2)

Here actual # of events is the number of events that would be produced for an integrated luminosity of 300 fb$^{-1}$. Note that the last line represents the fake photons that come from QCD processes, as described in 2.4.2. As can be seen the $Z^0Z^0 \rightarrow Z^0+Z^0$ and $WW \rightarrow Z^0+Z^0$ have a very small cross-section. In fact, they are so tiny for the given cuts (see section 3.2.1) that statistically, there will not be a single such event detected in ATLAS. These events are excluded as they will not contribute to any of the backgrounds. For most processes, an excess of events has been produced. The exceptions are $fg \rightarrow f+\gamma$ and $fg \rightarrow f+Z^0$ and the photon-jet confusion in the QCD background. However, this mixup of photons and jets is only considered for the $X \rightarrow \gamma\gamma$ channel. That these processes are underproduced can be motivated by the small contribution they add to the total background.

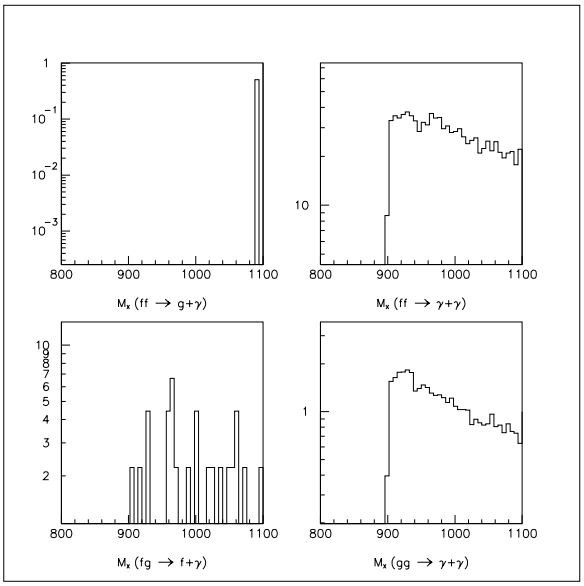


Figure 3.4: Histograms for the contributing backgrounds for the process $X \to \gamma\gamma$ for $m_X \sim$ 1000 GeV, after preselection cuts.

For the sake of completeness, all these backgrounds have been treated with all the selection criteria of the different processes of interest, see section 3.2.1. However, only a few of them will actually produce a background for a certain signal. These are the backgrounds presented in the figures.

### Background for $X \to \gamma\gamma$ at $m_X \sim 1$ TeV

The background of this process is presented in figure 3.4. The signals are normalized to an integrated luminosity of 300 fb$^{-1}$. We notice that the only processes that actually give a background are $\bar{f}f \to \gamma + \gamma$ and $gg \to \gamma + \gamma$. Even though their cross-sections are not so high, they have a final state that is irreducible. Hence, these are the two processes that we will keep when we calculate the backgrounds for different axion masses. Of these two, $\bar{f}f \to \gamma + \gamma$ is largest, which is only to expect in proton-proton collisions.

In addition to the direct backgrounds we have also simulated the QCD background to account for the possibility of confusion of a jet and a photon, as discussed in chapter 2.4.2. This is simulated just like all the other processes except that the cross-section is taken to be 3000 times[3] less (other-

[3]This is motivated by the result, which does not contain much background (figure 3.4).

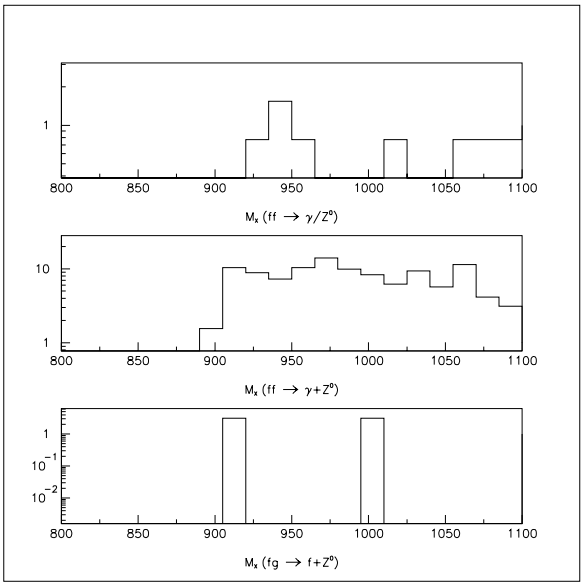


Figure 3.5: Histograms for the contributing backgrounds for the process $X \to Z^0\gamma \to l\bar{l}\gamma$ for $m_X \sim$ 1000 GeV, after preselection cuts.

wise the number of events would be enormous). When the selection criteria are applied, the invariant mass is calculated from the photon and jet with highest transverse momenta.

### Background for $X \to \gamma Z^0 \to \gamma\bar{l}l$ at $m_X \sim 1$ TeV

The background of this process is presented in figure 3.5. The signals are normalized to an integrated luminosity of 300 fb$^{-1}$ and the cuts (see section 3.2.1) have been applied. The only backgrounds that contribute to the signal are $\bar{f}f \to \gamma/Z^0$ and $\bar{f}f \to \gamma + Z^0$. These two signals will be kept for analysis of different axion masses. We do not consider the possible confusion of a jet with a photon because the probability of production of a $Z^0$ with the imposed cuts is very low in these processes. In analogy with the $X \to \gamma\gamma$ process, the $\bar{f}f \to \gamma + Z^0$ gives the irreducible background.

### Background for Other Processes at $m_X \sim 1$ TeV

As predicted in chapter 2, the background for axion decay to jets is tremendous, several order of magnitudes larger than the signals themselves. The one with lowest background (but still very large) is $X \to Z^0Z^0 \to jet+jet+$

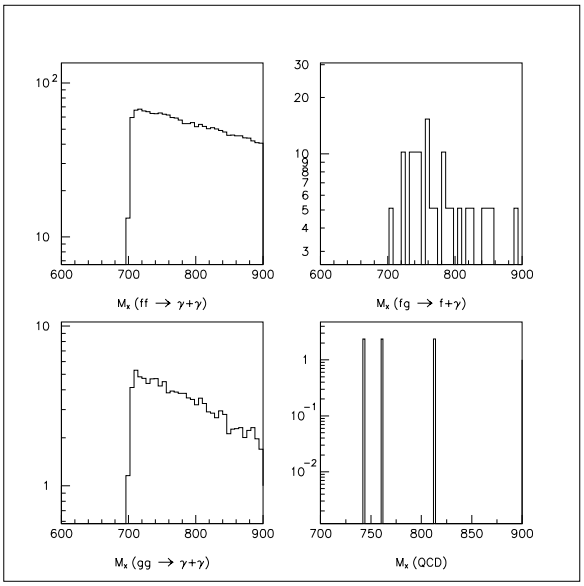


Figure 3.6: Histograms for contributing backgrounds for $X \to \gamma\gamma$ at $m_X \sim$ 800 GeV, after preselection cuts.

$\bar{l}l$, but unfortunately the cross-section is too small. Thus all final states that include jets are worthless for detecting the axion. The only process left, $X \to Z^0 Z^0 \to \bar{l}l\bar{l}l$ has a vanishing cross-section and will give about one event in 55 years of LHC operation at high luminosity (total: 6000 fb$^{-1}$).

### 3.2.3 Significant Background Processes for $m_X \sim 800$ GeV

The cross-sections are calculated with the two initial cuts, $p_T > 300$ GeV and $\sqrt{\hat{s}} > 700$ GeV (see section 3.2.1). The signals are normalized to an integrated luminosity of 300 fb$^{-1}$.

#### Background for $X \to \gamma\gamma$ at $m_X \sim 800$ GeV

As we found in section 3.2.2 there are only two important processes for $\gamma\gamma$ production. However, we have also considered the QCD background as this is known to increase dramatically for lower cuts. The result is presented in figure 3.6. Except for the lower cutoff in $\sqrt{\hat{s}}$, it is the same background as for the case of $m_X \sim 1000$ GeV.

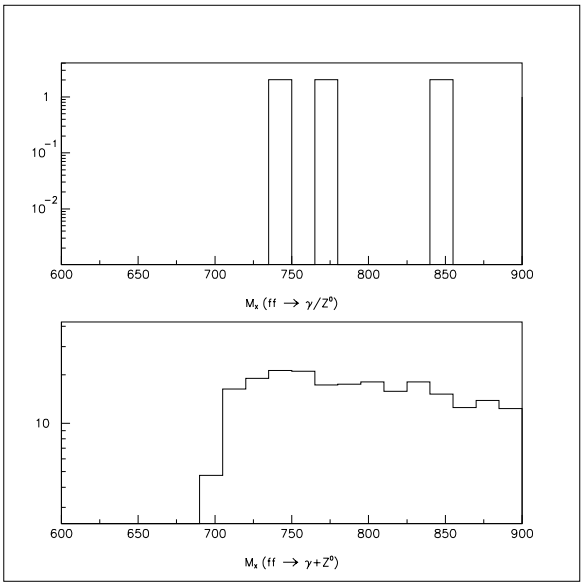


Figure 3.7: Histograms for contributing backgrounds for $X \to Z^0\gamma \to \bar{l}l\gamma$ at $m_X \sim 800$ GeV, after preselection cuts.

#### Background for $X \to \gamma Z^0 \to \gamma\bar{l}l$ at $m_X \sim 800$ GeV

As we found in section 3.2.2 there are only two important processes for $\gamma\bar{l}l$ production. The result is presented in figure 3.7. No spectacular deviations from the case $m_X \sim 1000$ GeV is noted.

#### Background for Other Processes at $m_X \sim 800$ GeV

For completeness, the other possible final states for axion decay should be considered also for this cut. Due to the weak signal of $Z^0Z^0$ production and the enormous background for $X \to \gamma Z^0 \to \gamma + jet + jet$ the above mentioned processes are the only ones that can be used for detection and identification of the hypercharge axion. If the integrated luminosity and the energy could be drastically increased they could be interesting, but in LHC they would hardly show up at all, as discussed in section 2.5.3.

## 3.3 Detection of the Hypercharge Axion in ATLAS

In this section we will study the two main decay channels of the axion, $X \to \gamma\gamma$ and $X \to \gamma Z^0 \to \gamma ll$. We will study the signals with the cuts

and apply the backgrounds to see whether the axion can be expected to be discovered. The condition for discovery will be that the signal should contain more events than five times the standard deviation of the background (i.e., five times the square-root of the number of background events in the mass-window), and that the number of events from the signal is $> 10$:

$$N_{ev} > 5 \times \sqrt{B} \quad \text{and} \quad N_{ev} > 10. \tag{3.3}$$

The ratio $N_{ev}/\sqrt{B}$ is called significance. The number of events is integrated between $m_X - 20$ GeV and $m_X + 20$ GeV. Note that the signal is expressed in units of $(\frac{\text{TeV}}{M_Y})^2$, which means that the signal will go down rapidly with increasing $M_Y$. Note that often in the theoretical models (see chapter 1) $M_Y \gg M_X$.

Two different masses of the axion are discussed, 800 GeV and 1000 GeV.

### 3.3.1 Signal and Background for $X \to \gamma\gamma$

For both masses, the signal is rather clean, and pretty strong.

For $m_X = 1$ TeV, the signal and the backgrounds are presented in figure 3.8 and we can clearly see the signal over the background. In the window $980 < m_X < 1020$ GeV we have about 204 background events and 210 signal events. This gives a significance of 14.7 sigma with $M_Y = 1$ TeV (see beginning of section).

For $m_X = 800$ GeV the number of events is higher but so is the background, as can be seen in figure 3.9. In the window $780 < m_X < 820$ GeV we have about 405 background events and 255 signal events. The significance is about 12.7 sigma, which means that the signal is possible to detect with $M_Y = 1$ TeV (see beginning of section). We remark that the background grows faster than the signal as the mass goes down.

### 3.3.2 Signal and Background for $X \to \gamma Z^0 \to \gamma \bar{l} l$

This signal is also clean. The only drawback is that the branching ratio for $Z^0 \to \bar{l} l$ is so low.

The background is very small for $m_X = 1$ TeV but so is the signal as can be seen in figure 3.10. In the window $980 < m_X < 1020$ GeV we have about 26 background events and 11.4 signal events. The signal is hardly above the background and we have a significance of 2.2 sigma for $M_Y = 1$ TeV (see beginning of section).

For a lower axion mass, $m_X = 800$ GeV, the signal is not clearly visible either (see figure 3.11). In the window $780 < m_X < 820$ GeV we have about

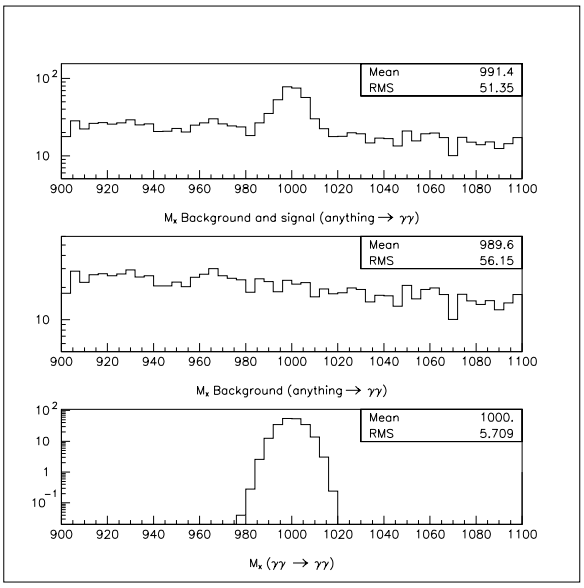


Figure 3.8: Histograms for signal and background for $X \to \gamma\gamma$ at $M_Y = 1000$ GeV, $m_X = 1000$ GeV, after preselection cuts.

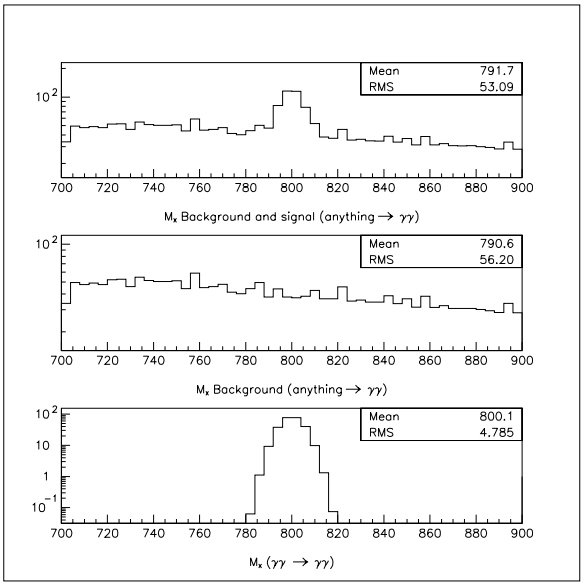


Figure 3.9: Histograms for signal and background for $X \to \gamma\gamma$ at $M_Y = 1000$ GeV, $m_X = 800$ GeV, after preselection cuts.

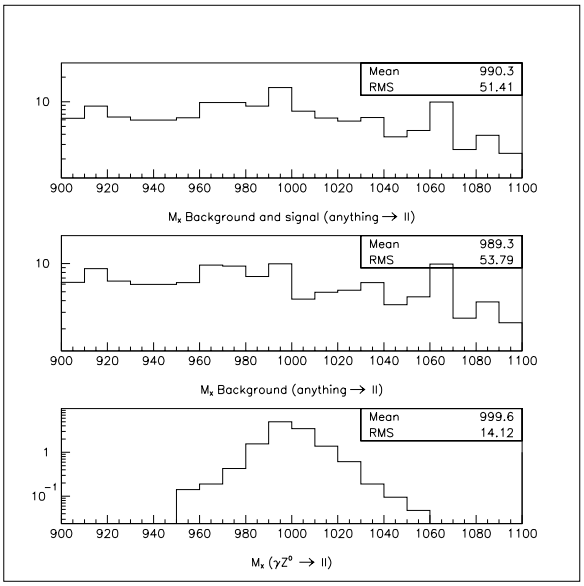


Figure 3.10: Histograms for signal and background for $X \to Z^0\gamma \to \bar{l}l\gamma$ at $M_Y = 1000$ GeV, $m_X = 1000$ GeV, after preselection cuts.

45 background events and 15 signal events. The significance is 2.2 sigma for $M_Y = 1$ TeV (see beginning of section).

## 3.4 Discussion and Conclusions

In the previous sections we have seen that there are basically two processes that can be used for detection of the hypercharge axion; $X \to \gamma\gamma$ and $X \to Z^0\gamma \to \bar{l}l\gamma$. The former signal has the higher signal-to-background ratio. In the case of $m_X = 800$ GeV and $M_Y = 1000$ GeV the axion would be observed (a 14.7 sigma significance). The other signal, $X \to Z^0\gamma \to \bar{l}l\gamma$, is more difficult to distinguish and for the same parameters we have a significance of 2.2 sigma. This is not enough for discovery, in the case of a clear signal for the $X \to \gamma\gamma$, but it could support a discovery and verify the branching ratios.

If we want to be certain that it is really the hypercharge axion that is detected, the branching ratios of $X \to \gamma\gamma$ and $X \to Z^0\gamma \to \bar{l}l\gamma$ have to be compared. The ratio $\Gamma_{\gamma\gamma}/\Gamma_{\bar{l}l\gamma}$ should be 28 for the hypercharge axion. The cross-section in itself cannot serve as a certain identification, though well as an indication, because the cross-section is proportional to $1/M_Y^2$ and

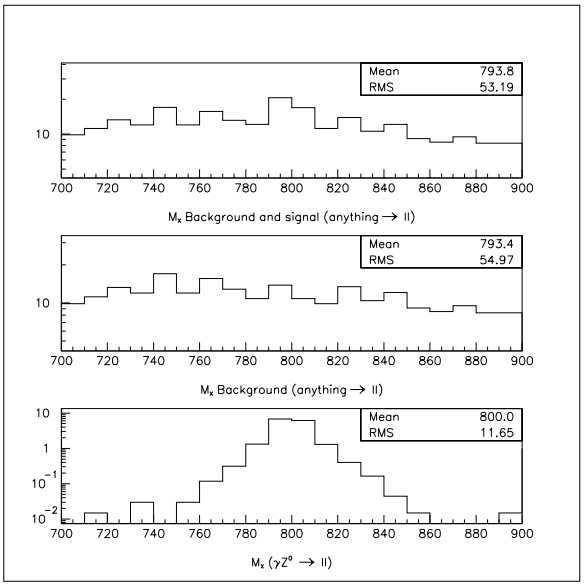


Figure 3.11: Histograms for signal and background for $X \to Z^0\gamma \to \bar{l}l\gamma$ at $M_Y = 1000$ GeV, $m_X = 800$ GeV, after preselection cuts.

$M_Y$ is an unknown parameter with dimension of mass. If all three decay channels are discovered, then it is a strong indication that we have discovered a pseudoscalar with the right coupling to the hypercharge. At that stage, the mass-scale $M_Y$ can be used to determine theoretically whether the pseudoscalar could amplify the hypermagnetic fields or not [17].

The scenario of $m_X = 800$ GeV and $M_Y = 1000$ GeV is taken from the article by Brustein and Oaknin [3], which gave the original idea of this thesis. The cross-sections in both their and our case are about 10 fb$^{-1}$.

There is also a theoretical argument why a particle in the mass region $300 < m_X < 1000$ GeV should be the hypercharge axion. It is not expected that there exist any particles in this mass range with electroweak couplings. The Higgs could in principle have this mass but this is outruled by the LEP (Large Electron Positron collider) high precision electroweak measurement. Furthermore, for a Higgs of this mass, the decay channel to two photons would be non-existent anyway. The Higgs would also have other, stronger, decay channels (like $W^+W^-$).

Note that in the calculations in this chapter, $M_Y$ is supposed to be 1 TeV, or, in other words, everything is expressed in terms of $(\frac{\text{TeV}}{M_Y})^2$. The parameter $M_Y$ is an energy scale, which is supposed to be much larger than

$m_X$ but in this thesis we disregard this to discover the limits of hypercharge axion detection in ATLAS. For $M_Y \lesssim 1.6$ TeV detection should be possible but hardly much above that. The precise limit depends on the mass of the axion too.

This thesis covers the possibility of discovering the hypercharge axion in ATLAS, but there are several points that could be elaborated and treated in more detail. Examples are the Weizsäcker-Williams approximation, the parton distribution functions and the amount of background produced. A study of processes and backgrounds could also be made for other values of the hypercharge axion mass.

There are also several questions in the theory behind the hypercharge axion that are still obscure. For example where the original hypermagnetic field came from and how enough $CP$ violation can be obtained.

# Appendix A

# Glossary

**Anomaly** An anomaly is the failure of a symmetry to survive renormalization.

**Antimatter** Antimatter is constituted of *antiparticles*.

**Antiparticle** An antiparticle is defined as having the opposite *quantum numbers* as the corresponding particle, but the same mass. Particles with their quantum numbers zero, except for spin which should be integer, (like the photon) are their own antiparticles. Experimentally there is no evidence for the effect of gravity on antimatter, but according to Einstein's principle of equivalence there should be no difference to matter. However, there are other possible theories, cousins of Einsteins theory of gravitation, that predict weaker gravity, or even inverse gravity for antiparticles. For a review of antiparticles, see, e.g., J. Eades and F. J. Hartmann, Rev. Mod. Phys. 1999 **71**, 373-420.

**Axial current** The axial current is defined as

$$A_\mu(x) = \bar{\psi}(x)\gamma_\mu\gamma_5\psi(x), \tag{A.1}$$

where $\psi(x)$ is the field at space-time point $x$, $\epsilon(x)$ is an arbitrary function of $x$ and $\gamma_\alpha$, $(\alpha = 1, 2, 3, 4, 5)$ are defined in appendix B.

**Baryogenesis** The generation of baryon asymmetry.

**Branching ratio** The relative probability that a particle will decay in a specific way. Example: $Z^0 \to e^+e^-$ has a branching ratio of about 3 percent. The sum of all branching ratios should be unity.

**Charge ($C$)** $C$ is an operation that reverses the charge of a particle.

**Chern-Simons number** A *winding number* for the electroweak Lagrangian. The change in Chern-Simons number is proportional to the change in baryon number, (see section 1.2.1).

**Decay channels** The possible decays of a particle.
Example:

$$Z^0 \to u\bar{u}, d\bar{d}, s\bar{s}, c\bar{c}, b\bar{b}, t\bar{t}, e^-e^+, \mu^-\mu^+, \tau^-\tau^+, \nu_e\bar{\nu}_e, \nu_\mu\bar{\nu}_\mu, \nu_\tau\bar{\nu}_\tau,$$

where the different processes have different *branching ratios*.

**Electroweak phase transition** The electroweak phase transition is when the electroweak symmetry is broken and the Higgs particle obtains a vacuum expectation value. It is estimated to have occurred about $10^{-10}$ s after big bang, when the temperature of the universe was $\sim 100$ GeV.

**Final state radiation** Final state radiation is decays of particles or emission of gluons or photons that occur after the event. In PYTHIA, this is the process that allow particle showers to evolve.

**Goldstone boson** A zero spin, zero mass particle associated with symmetry breaking.

**Higgs boson** A hypothetical particle required in the standard model of particle physics. The Higgs boson explains why $W^\pm$, and $Z^0$ have a mass.

**Initial state radiation** Initial state radiation is decays of particles or emission of gluons or photons that occur before the event.

**Massshell** On the mass shell means that the particle is real ($M^2 = E^2 - |\vec{p}|^2$). Off the mass shell means that it is virtual ($M^2 \neq E^2 - |\vec{p}|^2$).

**Parity ($P$)** Parity is an operation that gives a particle the same properties as if is was observed in a "point-like mirror". In other words, the spin of the particle will be inversed. $P\,|parity = p\rangle = |parity = -p\rangle$. The left-parity operator is represented by $P_L = \frac{1}{2}(1 - \gamma_5)$, where $\gamma_5$ is defined in appendix B. The right-parity operator is defined as $P_R = \frac{1}{2}(1 + \gamma_5)$.

**Sphaleron** An unstable solution of a partial differential equation. A sphaleron process is the process of passing a spahaleron, (see 1.2.1.)

**Symmetry** A symmetry operation does not change the physical solution. For example, the position of the origin in the coordinate system does not change the physical solution to problem.

**Winding number** A winding number is a characteristic that does not change during continuous transformations, if a certain point is avoided. A trivial example of this is found in complex analysis:

$$I(\gamma_{AB}, p) = \frac{1}{2\pi i} \int_{\gamma_{AB}} \frac{dz}{z - p} \tag{A.2}$$

where the value of the integral is independent of the curve $\gamma_{AB}$ as long as the points $A$ and $B$ are the same and $p$ is avoided.

The winding number is a sort of shortcut which lets us know the consequences of micro-level rules without elaborate calculations.

**Quantum numbers** The numbers that can be said to best describe the state of a particle. Examples: electric charge ($Q$), lepton number ($L$), baryon number ($B$), parity ($P$), spin ($S$), isospin ($I$), strangeness ($S$), and charge conjugation ($C$).

# Appendix B

# List of Symbols

## B.1 In Equations

| | |
|---|---|
| $X$ | Pseudoscalar axion |
| $m_X$ | Mass of the axion |
| $M_Y$ | Mass scale |
| $Y_{\mu\nu}$ | Hypercharge field strength (from $U(1)$) |
| $\tilde{Y}_{\mu\nu}$ | The dual of $Y_{\mu\nu}$, $\tilde{Y}_{\mu\nu} = \epsilon_{\alpha\beta\mu\nu}Y^{\alpha\beta}$ |
| $\epsilon^{\mu\nu\ldots}$ | The permutation symbol, defined as +1 for even permutationes of $\epsilon^{012\ldots}$ -1 for odd permutationes, and 0 for other values of the indices |
| $A_\mu$ | Hyperphoton vector |
| $Z_\mu$ | $Z^0$ vector |
| $m_Z$ | Mass of $Z^0$ |
| $H$ | Hamiltonian |
| $T$ | Temperature |
| $E$ | Energy |
| $B = n_B$ | $n_B = n_b - n_{\bar{b}}$, baryon number: difference between the number of baryons and antibaryons |
| $L$ | Lepton number |
| $s$ | Entropy |
| $\Gamma$ | Transition rate or branching ratio |
| $N_{CS}$ | Chern-Simons (winding) number |
| $S_E$ | Euclidian action |
| $H_Y$ | Hypermagnetic field |
| $E_Y$ | Hyperelectric field |
| $J_B$ | Baryon current |
| $\mu$ | Chemical potential |

| | |
|---|---|
| $\gamma$ | Photon |
| $l$ | Lepton |
| $g$ | Gluon |
| $\gamma$ | Photon |
| $f$ | Fermion (quark or lepton) |
| $q$ | Quark |
| $jet$ | Jet of particles, produced by a quark or a gluon |
| $t$ | Top quark |
| $b$ | Bottom quark |
| $p$ | Momentum |
| $p_T$ | Transverse momentum, $p_T \equiv \sqrt{p_x^2 + p_y^2}$ if $z$ is the beam direction |
| $\mathcal{L}$ | Luminosity |
| $\sigma$ | Cross-section |
| $t$ | Time |
| $n_f$ | Number of families of quarks/leptons, believed to be three |
| $i$ | Imaginary number, defined as $i^2 = -1$ |
| $\gamma$ matrices | $\gamma_0 = \begin{bmatrix} 1 & 0 & 0 & 0 \\ 0 & 1 & 0 & 0 \\ 0 & 0 & -1 & 0 \\ 0 & 0 & 0 & -1 \end{bmatrix}$ $\gamma_5 = \begin{bmatrix} 0 & 0 & 1 & 0 \\ 0 & 0 & 0 & 1 \\ 1 & 0 & 0 & 0 \\ 0 & 1 & 0 & 0 \end{bmatrix}$ $\gamma_1 = \begin{bmatrix} 0 & 0 & 0 & 1 \\ 0 & 0 & 1 & 0 \\ 0 & -1 & 0 & 0 \\ -1 & 0 & 0 & 0 \end{bmatrix}$ $\gamma_2 = \begin{bmatrix} 0 & 0 & 0 & -i \\ 0 & 0 & i & 0 \\ 0 & i & 0 & 0 \\ -i & 0 & 0 & 0 \end{bmatrix}$ $\gamma_3 = \begin{bmatrix} 0 & 0 & 1 & 0 \\ 0 & 0 & 0 & -1 \\ -1 & 0 & 0 & 0 \\ 0 & 1 & 0 & 0 \end{bmatrix}$ |

## B.2 List of Constants

| | | |
|---|---|---|
| $\theta_W$ | 28.7 degrees | The weak mixing angle $sin\theta_W \approx 0.23$ |
| $\hbar$ | $1.054571597\times10^{-34}$ Js | $\hbar = h/2\pi$, where $h$ is Planck's constant[1] |
| $c$ | 299792458 $ms^{-1}$ | Speed of light in vacuum[1] |
| $k_B$ | $1.3806503\times10^{-23}$ $JK^{-1}$ | Boltzmann's constant[1] |
| eV | $1.6022\times10^{-19}$ J | Electron Volt |

[1] Unless otherwise specified, we set $\hbar = c = k_B = 1$

## B.3 Abbreviations

| | |
|---|---|
| ATLAS | A Toroidal LHC ApparatuS |
| ATLFAST | A FORTRAN program to approximately simulate the ATLAS-detector |
| BAU | Baryon Asymmetry of the Universe |
| C | Charge-reverse operator |
| CERN | European laboratory for particle physics<br>(earlier: Conseil Européen pour la Recherche Nucléaire) |
| CP | Charge-Parity operator |
| CPT | Charge-Parity-Time operator |
| EW | Electro Weak |
| EWPT | Electro Weak Phase Transition |
| HCA | HyperCharge Axion |
| LHC | Large Hadron Collider |
| LEP | Large Electron Positron collider |
| LTU | Luleå University of Technology (in Swedish: Luleå Tekniska Universitet) |
| MSSM | Minimal Supersymmetric Standard Model |
| P | Parity operator |
| PYTHIA | A FORTRAN program to simulate collisions between particles |
| QCD | Quantum ChromoDynamics, the field theory for strong interactions |
| QED | Quantum ElectroDynamics, the field theory for electromagnetic interactions |
| SUSY | SUper SYmmetry |
| T | Time operator |

# Bibliography


[1] C. Nash, 1978, *Relativistic Quantum Fields*, Academic Press.

[2] M. E. Peskin, D. V. Schroeder, 1995, *An Introduction to Quantum Field Theeory*, Addison Wesley Publishing Company.

[3] R. Brustein and D. H. Oaknin, 1999, hep-ph/9906344.

[4] M. Trodden, 1999, Rev. Mod. Phys., **71**, 1463.

[5] G. Steigman, 1976, Ann. Rev. Astron. Astrophys. **14**, 336 (from [4]).

[6] F. W. Stecker, 1985, Nucl. Phys. **B252**, 25 (from [4]).

[7] A. G. Cohen, A. De Rújula, and S. L. Glashow, 1998, Astrophys. J. **495**, 539.

[8] A. D. Sakharov, 1967, Zh. Eksp. Teor. Fiz. Pis'ma Red. **5**, 32 [JETP Lett. **5**, 24 (1967)] (from [4]).

[9] E. W. Kolb and S. Wolfram, 1980, Nucl. Phys. **B172**, 224.

[10] P. T. Kabir, 1965, *Symmetries in Elementary Physics*, edited by A. Zichichi, Academic Press, New York.

[11] J. Eades and F. J. Hartman, 1999, Rev. Mod. Phys. **71**, 373.

[12] F. R. Klinkhammer and N. S. Manton, 1984, Phys. Rev. **D30**, 2212.

[13] G. D. Moore, C. Hu and B. Mueller, 1998, Phys. Rev. **D58**, 045001.

[14] R. D. Peccei and H. R. Quinn, 1977, Phys. Rev. **D16**, 1791
S. Weinberg, 1978, Phys. Rev. Lett. **40**, 223
M. Dine, 1981, Phys. Lett. **B104**, 199.

[15] M. Giovanni and M. E. Shaposhnikov, 1998, Phys. Rev. Lett. **80**, 22.

[16] R. Brustein and D. H. Oaknin, 1999, hep-ph/9901242.

[17] R. Brustein and D. H. Oaknin, 2000, hep-ph/00009009.

[18] E. Papageorgiu, 1995, Phys. Lett. **B352**, 394.

[19] T. Sjöstrand, 1994, Computer Physics Commun. **82**, 74.

[20] Particle Data Group, 2000, Eur. Phys. J. **C15**, 1.

[21] M. Gluck, E. Reya, and A. Vogt, 1990, Z. Phys. **C48**, 471.

[22] A. Djouadi, 1999, Int. J. Mod. Phys. **A10**, 1.

[23] ATLAS Detector & Physics Performance Technical Design Report, 1999, CERN/LHCC/99-14.